UDC 621.355
IRSTI 29.19.31

https://doi.org/10.55452/1998-6688-2026-23-2-381-391

[1]Kanatov Zh.S.,
PhD student, ORCID ID: 0009-0003-2975-0999,
kanatovzhantilek@gmail.com
[1*]Kalkozova Zh.K.,
Cand.Phys.-Math.Sc., Professor, ORCID ID: 0000-0002-4826-1678,
*e-mail: zhanar.kalkozova@kaznu.edu.kz
[2]Mukash Zh.O.,
PhD, Assistant Professor, ORCID ID: 0009-0004-7713-3925,
e-mail: zhanar.mukash@sdu.edu.kz
[3]Mirzaeian M.,
PhD, ORCID ID: 0000-0002-1474-8330,
e-mail: mojtaba.mirzaeian@uws.ac.uk
[1]Abdullin Kh.A.
Dr.Phys.-Math.Sc., Professor, ORCID ID: 0000-0002-2729-2272,
e-mail: kh.abdullin@physics.kz

[1]National Nanotechnology Laboratory of Open Type of Al–Farabi Kazakh National University, Almaty, Kazakhstan
[2]School of Education and Humanities, SDU University, Kaskelen, Kazakhstan
[3]School of Computing, Engineering and Physical Sciences, University of the West of Scotland, Paisley, United Kingdom

SURFACE TRANSFORMATION AND ENHANCED ELECTROCHEMICAL PERFORMANCE OF Ni_3S_2/NI FOAM ELECTRODES FOR HYBRID SUPERCAPACITORS

Abstract

The process of sulfurization of nickel foam surfaces to obtain Ni_3S_2 layers with high electrochemical capacitance and stability during electrochemical cycling has been extensively studied. However, the role of nickel hydroxide layers, which are expected to form under the electrochemical operating conditions of the Ni_3S_2/NF electrode, has not been sufficiently investigated. In the present work, it is demonstrated that the hydroxide phase makes a significant contribution to both electrochemical capacitance and cyclic stability. The Ni_3S_2/NF electrode was fabricated via a single–step hydrothermal method in the presence of thiourea at 160 °C. The initial structure of Ni_3S_2 on the NF surface was subsequently modified through electrochemical cycling in a KOH electrolyte. The increase in electrochemical capacitance of the electrode was accompanied by the formation of multiple nickel hydroxide phases, as identified by X–ray diffraction (XRD) and Raman spectroscopy. The electrode exhibited high performance stability over 20,000 galvanostatic charge–discharge (GCD) cycles at a current density of 20 A g^{-1}, retaining 90% of its maximum capacitance. The specific capacitance of the Ni_3S_2 electrode was 758 F g^{-1} at a current density of 2.7 A g^{-1}. When the current density increased to 90 A g^{-1}, the specific capacitance decreased to 233 F g^{-1}, corresponding to 30% of the capacitance at 2.7 A g^{-1}.

Keywords: Ni_3S_2, nickel foam, hybrid supercapacitor, nickel hydroxide, electrochemical activation, cycling stability.

Received April 7, 2026; accepted May 27, 2026.

Introduction

Renewable energy relies on inherently unstable energy sources. The development of reliable energy systems therefore requires advanced energy storage technologies. Supercapacitors, characterized by high energy efficiency, represent an important component of such systems, providing smoothing of power consumption fluctuations and thereby enhancing the stability of energy systems [1–3]. The main types of electrochemical supercapacitors used for energy storage include electrical double–layer capacitors (EDLCs), pseudocapacitors, and hybrid supercapacitors. Hybrid electrochemical supercapacitors combine the advantages of high specific power, enhanced specific energy, and long service life, integrating the properties of electrical double–layer capacitors and pseudocapacitors to achieve efficient energy storage.

The most promising materials for hybrid electrochemical supercapacitors include carbon nanomaterials (graphene, carbon nanotubes), transition metal oxides (MnO_2, NiO), conductive polymers (polyaniline, polypyrrole), and their composites [4–7]. Metal sulfides, such as Ni_3S_2 and NiS, are also considered promising materials for hybrid electrochemical supercapacitors due to their high specific capacitance, good electrical conductivity, and structural stability associated with their layered structure and the ability to undergo reversible redox reactions.

Compared with metal oxides, metal sulfides exhibit several advantages in hybrid electrochemical supercapacitors, including higher electrical conductivity, enhanced specific capacitance due to rich redox activity and layered structure, as well as improved mechanical stability during cycling, which contributes to increased durability and efficiency.

Many metal oxides are dielectric in nature. In contrast, sulfides generally exhibit higher electrical conductivity than oxides, which facilitates electron transfer, reduces internal resistance, and increases specific power [8]. Sulfides also demonstrate enhanced redox activity due to the presence of a greater number of redox–active centers and weaker metal–sulfur (M–S) bonds. As a result, they enable more extensive Faradaic redox reactions, associated with the multiple valence states of metals and the lower electronegativity of sulfur compared to oxygen, leading to higher specific capacitance.

The structural flexibility of sulfides contributes to improved mechanical stability during charge–discharge cycling, resulting in enhanced cyclic stability and improved energy storage performance. Furthermore, sulfides combined with oxides or carbon–based materials often outperform electrodes based solely on oxides, owing to synergistic effects that enhance ion transport and increase the active surface area.

Nickel sulfides (e.g., NiS, Ni_3S_2) are particularly promising for hybrid electrochemical supercapacitors due to their superior electrical conductivity compared to nickel oxides, which provides faster electron transfer and higher power density. In addition, their stable crystal structures, such as the layered morphology of NiS, provide excellent cyclic stability, maintaining performance over thousands of charge–discharge cycles. These characteristics, together with their cost–effectiveness and relative ease of synthesis, make nickel sulfides attractive electrode materials for efficient and durable hybrid supercapacitors.

Among nickel sulfides, Ni_3S_2 [9] is especially promising due to its high specific capacitance, good electrical conductivity, and structural stability. Ni_3S_2 exhibits a balanced combination of redox properties, while its developed morphology provides a high active surface area and facilitates ion diffusion, making it suitable for the fabrication of high–performance supercapacitors.

However, under electrochemical conditions in an alkaline environment, Ni_3S_2 can undergo oxidation at high positive potentials according to the reaction:

$$Ni_3S_2 + 6OH^- \rightarrow 3Ni(OH)_2 + 2S^{2-}$$

resulting in the formation of nickel hydroxide phases. Since these phases exhibit high electrochemical activity and possess high specific capacitance, their formation must be taken into account. However, to the best of our knowledge, this aspect of Ni_3S_2/NF electrode modification has been investigated in only two studies [10,11]. In [10], the Ni_3S_2 layers were obtained by annealing, not by the hydrothermal method. In Ref. [11], the Ni_3S_2/NF electrode was synthesized via a rapid hydrothermal

method in the presence of a nickel salt in the growth solution, which reduced the synthesis time to approximately 3 h.

In the present study, phase transformations in Ni_3S_2/NF electrodes obtained using the conventional method [9, 12] of nickel foam sulfidation in thiourea are investigated.

Material and methods

Thiourea (CH_4N_2S) and nickel foam (NF) with a thickness of 1.5 mm (Shenzhen Tianchenghe Technology Co., Ltd.) and an areal density of 0.03 g cm^{-2} were used as starting materials. Milli–Q water (18.2 MΩ·cm) was obtained using an AQUAMAX–Ultra 370 series water purification system (YL Instrument Co., Anyang, Korea).

Prior to hydrothermal synthesis, the NF substrates were purified by ultrasonic treatment in a 1 M HCl solution. The substrate was then placed in a Teflon beaker, and 30 mL of a 1 mM thiourea solution was added. The hydrothermal reactor with a Teflon liner was sealed and placed in an oven at 160 °C for 24 h.

After synthesis and cooling to room temperature, the autoclave was removed from the furnace. The solution remained transparent after synthesis, and the resulting layers were dense and mechanically stable. The NF sample was rinsed with water, subjected to ultrasonic treatment for 30 min, and subsequently dried.

The surface morphology of the samples was examined using a Quanta 200i scanning electron microscope (FEI). X–ray diffraction (XRD) measurements were carried out using a MiniFlex diffractometer (Rigaku) with Cu Kα radiation (λ = 1.5418 Å). Raman spectra were recorded using an NTEGRA spectrometer (NT–MDT, Zelenograd, Russia) with an excitation wavelength of 473 nm.

The electrochemical performance of the Ni_3S_2/NF electrodes was investigated in a three–electrode configuration using a large–area carbon counter electrode and an Ag/AgCl reference electrode. Electrochemical measurements were performed using a CorrTest CS2350 bipotentiostat (Wuhan Corrtest Instruments Corp., Ltd., Wuhan, China), including cyclic voltammetry (CV), galvanostatic charge–discharge (GCD), and electrochemical impedance spectroscopy (EIS). The capacitance was calculated from CV and GCD measurements using Eqs. (1) and (2), respectively:

$$C = \frac{1}{2\nu(U_{max}-U_{min})}\oint I(V)\,dV, \quad (1)$$

$$C = \frac{I\Delta t}{\Delta U}, \quad (2)$$

where ν (V s^{-1}) is the scan rate, and U_{max} −U_{min} (V) is the potential window in the CV measurements. The current I(V) is integrated over the full CV cycle. For GCD measurements, the capacitance was determined from the discharge current I (A), discharge time Δt (s), and voltage drop ΔU (V). To determine the specific capacitance, the mass of the NF samples was measured before and after synthesis. The areal mass of the initial nickel foam was approximately 0.0314 g cm^{-2}. Under the selected synthesis conditions, the mass increase for a sample area of 1 cm^2 was 1.2 mg cm^{-2}. Since the Ni_3S_2 layer is formed as a result of nickel sulfidation, the mass of the synthesized Ni_3S_2 on the NF substrate was estimated to be 4.5 mg cm^{-2}.

Results

Scanning electron microscopy (SEM) micrographs reveal the evolution of the Ni_3S_2/NF electrode surface before and after cyclic voltammetry (CV). The initial morphology is characterized by thin, interwoven nanosheets forming an open porous structure, which provides a high specific surface area and facilitates electrolyte access to active sites.

After intensive electrochemical cycling in an alkaline medium within the potential range from −0.5 to 1 V, noticeable morphological changes are observed. The structural features become less distinct, appearing blurred, which may be attributed to the formation of new phases with dimensions

below the resolution limit of the microscope. During electrochemical oxidation and hydration, a nanocrystalline layer of nickel oxides/hydroxides forms on the surface of the sulfide, as confirmed by X–ray diffraction (XRD) data.

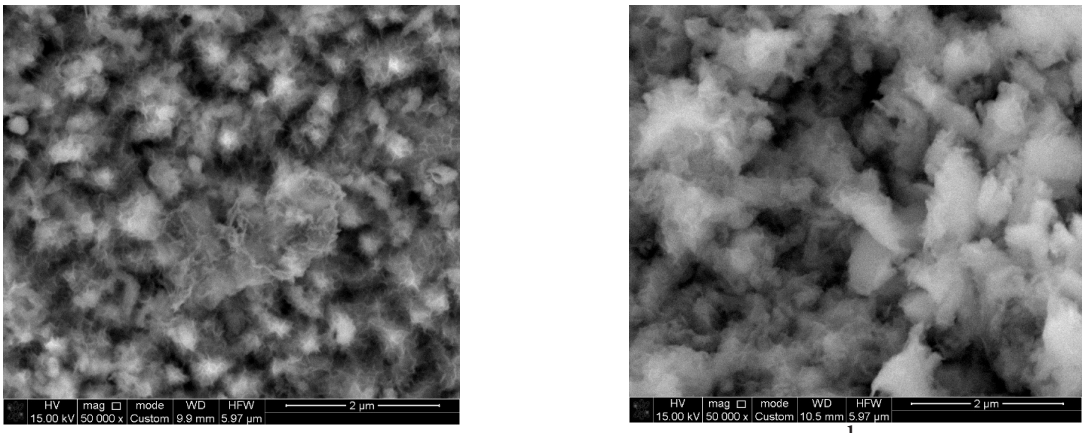

a b

Figure 1 – SEM images of Ni_3S_2 layers on nickel foam grown by the hydrothermal method: a – after synthesis, b – after CV measurements in 3M KOH in the range of –0.5 V to +1 V vs Ag/AgCl

Figure 2 presents XRD patterns of the sample after synthesis (curve 1), after approximately 100 CV cycles and stabilization of the CV curves in a 3 M KOH electrolyte (curve 2), and after 20,000 GCD cycles (curve 3). The initial sample exhibits well–defined diffraction peaks corresponding to the crystalline Ni_3S_2 phase (JCPDS No. 01–073–0698), confirming the formation of nickel sulfide on the substrate. Intense peaks at 44.5°, 51.8°, and 76.3° are attributed to metallic nickel (Ni) from the NF substrate. After CV cycling in the potential range of −0.5 to +1 V (curve 2), the intensity of the Ni_3S_2 peaks decreases, and new diffraction maxima characteristic of hydrated nickel hydroxide appear. This indicates effective surface oxidation of the sulfide during redox processes over a wide potential window. After 20,000 GCD cycles (curve 3), the contribution of Ni_3S_2 decreases further, indicating an increase in the thickness of the nickel hydroxide layer. Additionally, significant broadening of the nickel hydroxide peaks is observed, suggesting a reduction in the crystallite size as a result of repeated Faradaic reactions.

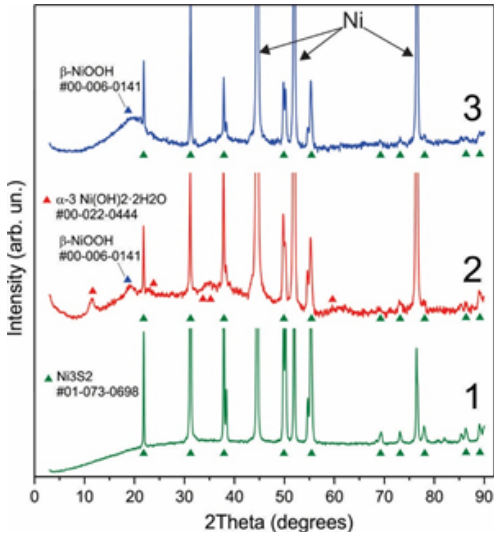

Figure 2 – XRD patterns of the electrode: 1 − initial (pristine) electrode, 2 − after cyclic voltammetry (CV) measurements in 3 M KOH in the potential range from −0.5 V to +1 V vs. Ag/AgCl, and 3 − after 20,000 galvanostatic charge–discharge (GCD) cycles in 3 M KOH in the potential range from 0 V to 0.5 V vs. Ag/AgCl

Raman spectroscopy was employed to identify the composition of the electrode surface before and after electrochemical measurements, which is particularly important for detecting thin layers of amorphous and nanocrystalline phases that are not observable by XRD. Figure 3 (curve 1) shows the Raman spectrum of the as–synthesized sample. The spectrum is characterized by a set of peaks in the region corresponding to the characteristic vibrational modes of the Ni_3S_2 crystal lattice. The main peaks are located at 145, 200, 245, 305, and 348 cm^{-1}, which is in good agreement with literature data for the Ni_3S_2 phase [13]. After short–term CV measurements (40–50 cycles) in 3 M KOH within the potential range from −0.5 to +1 V vs Ag/AgCl, the Raman spectrum undergoes significant changes (curve 2). The peaks corresponding to nickel sulfide almost completely disappear, while two broad bands centered at approximately 480 cm−1 and 560 cm^{-1} become dominant. These bands are attributed to vibrational modes associated with nickel oxyhydroxide (NiOOH) [14–17].

The obtained results confirm that, during deep anodic polarization (up to 1 V vs Ag/AgCl), the Ni_3S_2 surface undergoes irreversible electrochemical transformation. The formation of $Ni(OH)_2$/NiOOH phases indicates the development of a reaction layer on the sulfide surface, which provides Faradaic charge storage processes in an alkaline electrolyte.

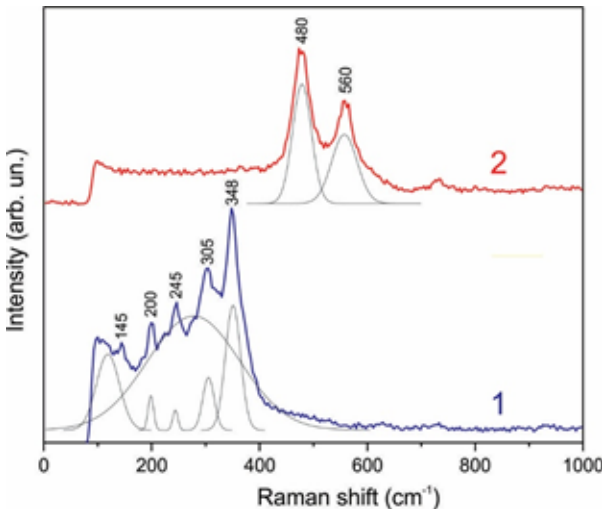

Figure 3 – Raman spectra of Ni_3S_2 layers on nickel foam: curve 1 − after synthesis, and curve 2 − after cyclic voltammetry (CV) measurements in 3 M KOH in the potential range from −0.5 V to +1 V vs. Ag/AgCl

Prior to the investigation of the long–term stability of the Ni_3S_2/NF electrode, a preliminary activation procedure was carried out. It should be noted that the initial capacitance of the electrode immediately after synthesis was low. During the initial CV cycles, the current response gradually increased, and after approximately 50–80 cycles, the CV curves reached a stable state. This behavior may be attributed to the gradual penetration of the electrolyte into the porous structure, the formation of electrochemically active sites, and partial surface oxidation.

The long–term stability of the Ni_3S_2/NF electrode was evaluated by galvanostatic charge–discharge (GCD) cycling over 20,000 cycles in a 3 M KOH electrolyte within the potential range of 0–0.5 V vs Ag/AgCl. Figure 4a shows the dependence of capacitance and Coulombic efficiency on the number of cycles, while Figure 4b presents a comparison of GCD charge–discharge curves at a current of 100 mA at the initial stage and after 20,000 cycles.

The cycling data reveal a characteristic process of continued, but slower, electrode activation during the first 2000 cycles, during which the areal capacitance increases from approximately 3.5 to 5.2 F cm^{-2}.

Considering that Raman spectroscopy results indicate rapid modification of the Ni_3S_2 surface layer, this increase in capacitance can be attributed to the formation of an electrochemically active

$Ni(OH)_2$/NiOOH layer. After approximately 2000 cycles, the electrode exhibits stabilization of its electrochemical properties and demonstrates exceptional cyclic stability. Even after 20,000 cycles, no decrease in capacitance or increase in series resistance is observed. The Coulombic efficiency remains stable at a value close to 100%, confirming the high reversibility of the Faradaic reactions.

The GCD curves recorded at the initial stage and after 20,000 cycles exhibit nearly identical shapes with pronounced voltage plateaus (Figure 4b), which is characteristic of battery–type behavior. A significant increase in charge and discharge times for the 20,000th cycle compared to the initial cycle confirms the increase in capacitance resulting from surface activation. At the same time, the preservation of curve symmetry indicates that the internal resistance (IR drop) of the electrode does not increase significantly over the entire cycling period.

Figures 5 and 6 present the GCD and CV characteristics of the electrode after 20,000 cycles, while Figure 7 shows the electrochemical impedance spectroscopy (EIS) results. At a low current density of 0.22 A g^{-1}, the capacitance of the electrode with an area of 1 cm^2 reaches 3.8 F, which, considering the mass loading of 4.5 mg cm^{-2}, corresponds to a specific capacitance of 853 F g^{-1}.

At an operating current density of 2.7 A g^{-1}, the specific capacitance is 758 F g^{-1}, and when the current density increases to 90 A g^{-1}, the specific capacitance decreases to 233 F g^{-1}, corresponding to 30% of the capacitance at 2.7 A g^{-1}. This indicates that the electrode retains a high specific capacitance even at high current densities.

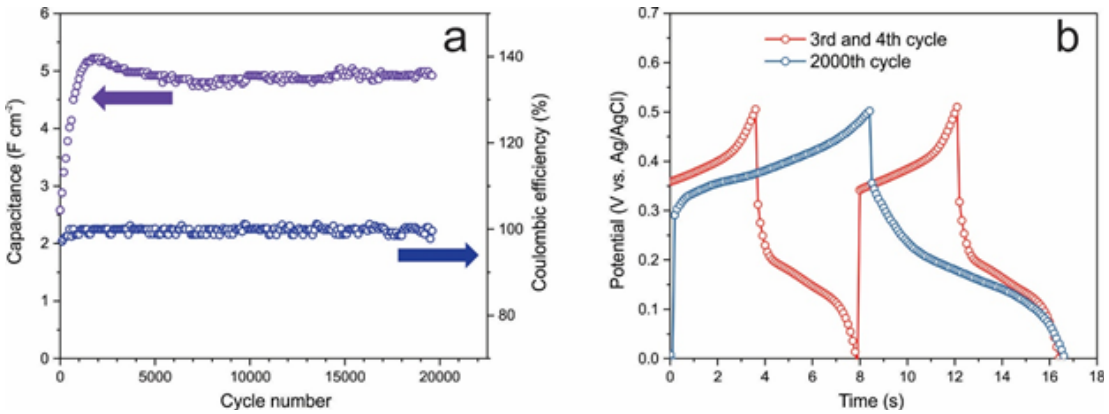

Figure 4 – (a) Capacitance and Coulombic efficiency of the Ni_3S_2/NF electrode as a function of cycle number; (b) comparison of galvanostatic charge–discharge (GCD) curves at a current of 100 mA (22 A g^{-1}) at the beginning of cycling and after 20,000 cycles in 3 M KOH in the potential range of 0 V to 0.5 V vs. Ag/AgCl

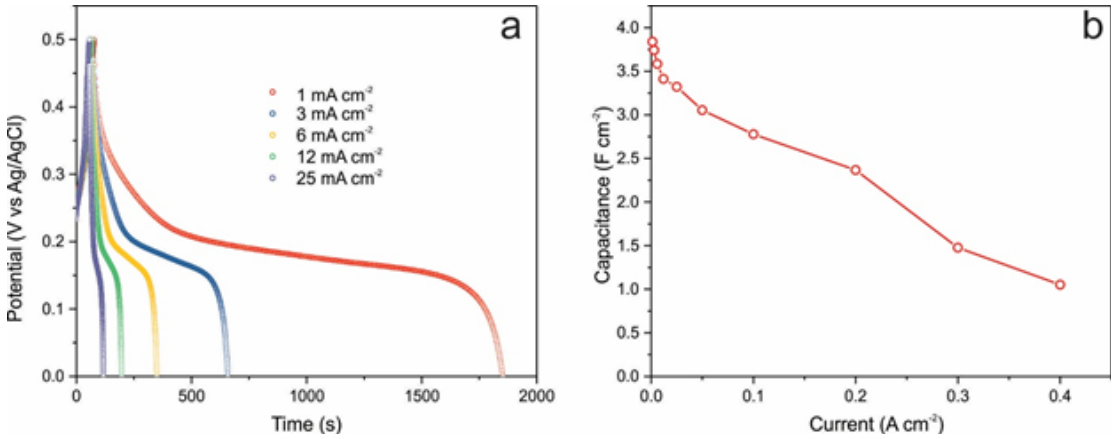

Figure 5 – (a) Galvanostatic charge–discharge (GCD) curves at different discharge current densities (charge current density fixed at 25 mA cm^{-2} for all curves); (b) specific capacitance as a function of discharge current density.

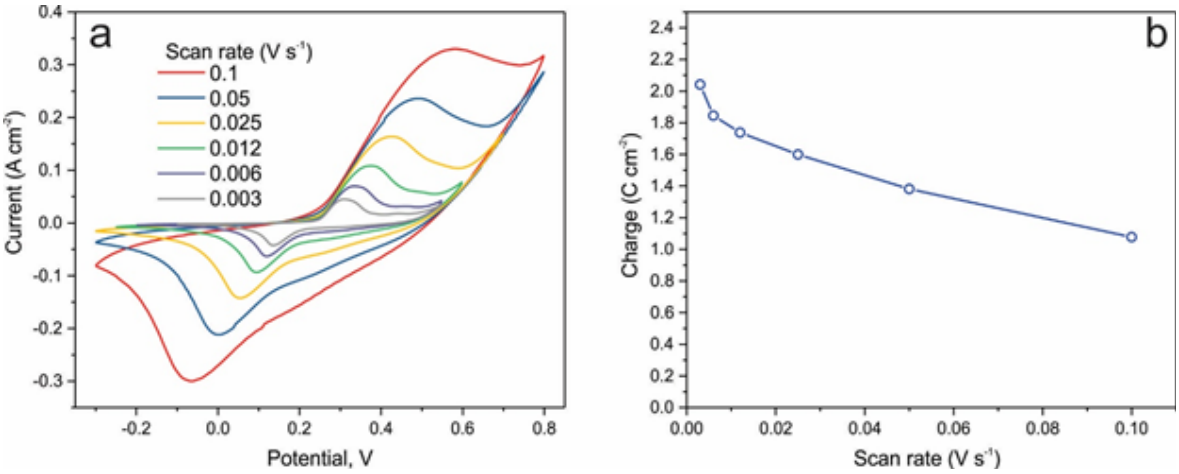

Figure 6 – (a) Cyclic voltammetry (CV) curves at different scan rates;
(b) specific capacitance as a function of scan rate.

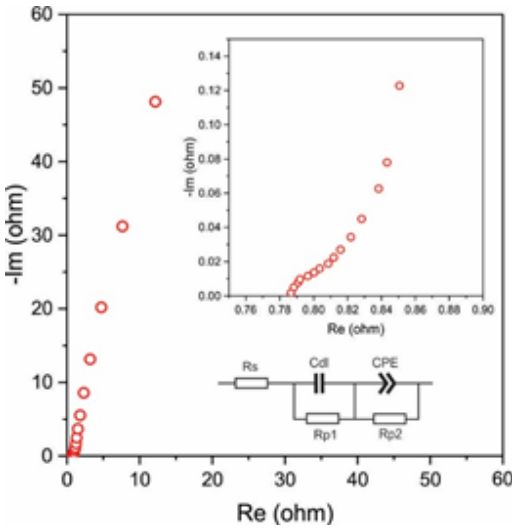

Figure 7 – Nyquist plot of the Ni_3S_2/NF electrode after 20,000 cycles.
Electrochemical impedance spectroscopy (EIS) measurements were performed
in the frequency range from 50 kHz to 0.0016 Hz at a DC offset of 300 mV vs. Ag/AgCl.
The inset shows the equivalent circuit model of the electrode.

Discussion

The results of the study demonstrate that the high electrochemical performance and stability of the Ni_3S_2/NF electrode are due to the phase and structural transformations of its surface during operation.

The phase transformation of the surface is confirmed by Raman spectroscopy. The spectra (Figure 3) show the disappearance of the characteristic vibrational modes of the Ni_3S_2 crystal lattice after electrochemical activation. Instead, bands at approximately 480 cm^{-1} and 560 cm^{-1}, corresponding to stable nickel oxyhydroxide (NiOOH) phases, become dominant, indicating the formation of an electrochemically active reaction layer.

The structural transformation is supported by SEM and XRD data. Even relatively short–term CV cycling leads to a reduction in the contribution of the Ni_3S_2 phase and the appearance of new diffraction maxima characteristic of hydrated nickel hydroxide.

Prolonged cycling results in the formation of β–$Ni(OH)_2$ nanoparticles. Significant broadening of the diffraction peaks after 20,000 cycles indicates a decrease in crystallite size, which increases the active surface area and promotes Faradaic reactions.

As a consequence of these phase and structural transformations, the electrode demonstrates exceptional durability, retaining more than 90% of its maximum capacitance after 20,000 GCD cycles. The activation process during the first 2000 cycles, accompanied by an increase in capacitance from 3.5 to 5.2 F cm^{-2}, is directly associated with the formation of a developed $Ni(OH)_2$/NiOOH layer. The stability of the Coulombic efficiency at approximately 100% further confirms the high reversibility of the redox processes in the formed nanostructure.

Thus, the high capacitance and stability of the electrode are ensured by synergistic interaction between the conductive Ni_3S_2/NF framework and the nanocrystalline nickel hydroxide/oxyhydroxide layer formed under electrochemical conditions, which remains electrochemically active and mechanically stable over tens of thousands of cycles.

Conclusion

In this work, an electrode based on Ni_3S_2 nickel sulfide on nickel foam was synthesized using a simple one–step hydrothermal method. This approach is well established in the literature and has proven to be effective for the fabrication of electrodes for hybrid supercapacitors. However, despite numerous studies on the properties of Ni_3S_2 supercapacitor electrodes grown on NF via thiourea–assisted sulfidation, the role of nickel hydroxide layers formed under electrochemical conditions on the surface of Ni_3S_2 has not been sufficiently addressed.

For comparison, in Ref. [10], Ni_3S_2 electrodes were prepared by annealing an NF substrate in an H_2S–containing atmosphere (5% H_2S–95% N_2) at 400 °C for 60 min. In Ref. [11], nickel acetate was introduced into the growth solution to accelerate synthesis, reducing the processing time to approximately 3 h. However, the results obtained in the present study differ significantly from those reported in Ref. [11], particularly in terms of the superior stability of electrochemical performance during cycling.

It has been demonstrated that robust Ni_3S_2 layers obtained by sulfidation of NF in thiourea undergo surface modification during electrochemical activation in an alkaline medium, resulting in the formation of an active layer composed of nanocrystalline $Ni(OH)_2$ phases and stable NiOOH species. This composite structure provides high specific capacitance and excellent cycling stability.

The obtained results highlight the critical role of the synergistic interaction between the conductive sulfide framework and the nanocrystalline hydroxide/oxyhydroxide layer. This synergy makes the $Ni(OH)_2$/Ni_3S_2/NF system a promising electrode material for long–life hybrid supercapacitors.

Acknowledgements

The study was carried out with the financial support of the Ministry of Science and Higher Education of the Republic of Kazakhstan (grant No AP23488976).

REFERENCES

1 Lakshmi, K.C.S., Vedhanarayanan, B. High–Performance Supercapacitors: A Comprehensive Review on Paradigm Shift of Conventional Energy Storage Devices. Batteries, 9(4), 202 (2023). https://doi.org/10.3390/batteries9040202.

2 Nargish Parvin, Dhananjaya Merum, Misook Kang, Sang Woo Joo, Jae Hak Jung and Tapas Kumar Mandal. Recent advances in hybrid supercapacitors: a review of high performance materials and scalable fabrication techniques. Journal of Materials Chemistry A, 13(30), 24320–24386 (2025). https://doi.org/10.1039/D5TA02887F.

3 Neeraj Singh, Virendra Singh, Neeraj Bisht, Puneet Negi, Archana Dhyani, Rajat Kumar Sharma, Tewari B.S. A comprehensive review on supercapacitors: Basics to recent advancements. Journal of Energy Storage. 121, 116498 (2025). https://doi.org/10.1016/j.est.2025.116498.

4 Reenu, Sonia, Lakshita Phor, Ashok Kumar, Surjeet Chahal, Electrode materials for supercapacitors: A comprehensive review of advancements and performance. Journal of Energy Storage. 84, Part B, 110698 (2024). https://doi.org/10.1016/j.est.2024.110698.

5 Mojtaba Mirzaeian, Qaisar Abbas, Abraham Ogwu, Peter Hall, Mark Goldin, Marjan Mirzaeian, Hassan Fathinejad Jirandehi. Electrode and electrolyte materials for electrochemical capacitors. International Journal of Hydrogen Energy. 42, 25565–25587 (2017). https://doi.org/10.1016/j.ijhydene.2017.04.241.

6 Muhammad Faisal Iqbal, Farooq Nasir, Fiza Shabbir, Zaheer Ud Din Babar, Muhammad Farooq Saleem, Kaleem Ullah, Nana Sun, Faizan Ali. Supercapacitors: An Emerging Energy Storage System. Advanced Energy and Sustainability Research. 6, 2400412 (2025). https://doi.org/10.1002/aesr.202400412.

7 Ander González, Eider Goikolea, Jon Andoni Barrena, Roman Mysyk. Review on supercapacitors: Technologies and materials. Renewable and Sustainable Energy Reviews. 58, 1189–1206 (2016). https://doi.org/10.1016/j.rser.2015.12.249.

8 Mengkang Zhu, Dan Wang, Zongyu Ge, Lin Pan, Yanli Chen, Wenchang Wang, Naotoshi Mitsuzaki, Shuyong Jiad Zhidong Chen. Recent advances in transition metal sulfide–based electrode materials for supercapacitors. Chemical Communications. 61, 8314–8326 (2025). https://doi.org/10.1039/D5CC01411E.

9 Dhakal, G., Sahoo, S., Sharma, K.P., Zhao, G.–L. A Review on the Recent Advancements of Ni–Based Sulfides and Mixed Sulfides for Supercapacitors and Electrocatalysis (Oxygen Evolution Reaction). Molecules. 30, 2877 (2025). https://doi.org/10.3390/molecules30132877.

10 Yan–Qiang Cao, Xu Qian, Wei Zhang, Min Li, Shan–Shan Wang, Di Wu, Ai–Dong Li. Self–formed porous Ni(OH)2 on Ni3S2/Ni foam during electrochemical cycling for high performance supercapacitor with ultrahigh areal capacitance. Electrochimica Acta. 303, 148–156 (2019). https://doi.org/10.1016/j.electacta.2019.02.075.

11 Abdullin K.A., Gabdullin M.T., Gritsenko L.V., Kalkozova Zh.K., Kanatov Zh.S., Markhabayeva A.A., Nemkayeva R.R., Zhapargali D., Mirzaeian M. In situ formation of nanocrystalline $Ni(OH)_2$ in alkaline electrolyte explains superior capacitance and cycling stability of Ni_3S_2/NF electrodes. Scientific Reports (2026). https://doi.org/10.1038/s41598–026–42576–y

12 Xuerui Yi, Caroline Kirk, and Neil Robertson. Achieving Complete Conversion from Nickel Foam to Nickel Sulfide Foam for a Freestanding Hybrid–Supercapacitor Electrode. ChemElectroChem. 11, e202400383, (2024). https://doi.org/10.1002/celc.202400383 .

13 Jeng–Han Wang, Zhe Cheng, Jean–Luc Brédas, Meilin Liu. Electronic and vibrational properties of nickel sulfides from first principles. Journal of Chemical Physics. 127, 214705 (2007). https://doi.org/10.1063/1.2801985.

14 Julia Gallenberger, Harol Moreno Fernández, Achim Alkemper, Mohan Li, Chuanmu Tian, Bernhard Kaisera, Jan Philipp Hofmann. Stability and decomposition pathways of the NiOOH OER active phase of NiOx electrocatalysts at open circuit potential traced by ex situ and in situ spectroscopies. Catalysis Science & Technology. 13, 4693–4700 (2023). https://doi.org/10.1039/d3cy00674c.

15 Robert Kostecki, Frank McLarnon. Electrochemical and In Situ Raman Spectroscopic Characterization of Nickel Hydroxide Electrodes: I. Pure Nickel Hydroxide. Journal of the Electrochemical Society. 144, 485 (1997). https://doi.org/10.1149/1.1837437.

16 Hall D.S., Lockwood D.J., Bock C., MacDougall B.R. Nickel hydroxides and related materials: a review of their structures, synthesis and properties. Proceedings of the Royal Society A. 471, 20140792 (2015). http://dx.doi.org/10.1098/rspa.2014.0792.

17 Minjeong Lee, Yeongeun Jang, Gayoung Yoon, Seonghwa Lee, Gyeong Hee Ryu. Synthesis and electrochemical evaluation of nickel hydroxide nanosheets with phase transition to nickel oxide. RSC Advances. 14, 10172 (2024). https://doi.org/10.1039/d4ra01120a.

[1]Қанатов Ж.С.,
докторант, ORCID ID: 0009-0003-2975-0999,
kanatovzhantilek@gmail.com
[1*]Калкозова Ж.К.,
ф.-м.ғ.к., профессор, ORCID ID: 0000-0002-4826-1678,
*e-mail: zhanar.kalkozova@kaznu.edu.kz
[2]Мұқаш Ж.О.,
PhD, ассистент профессор, ORCID ID: 0009-0004-7713-3925,
e-mail: zhanar.mukash@sdu.edu.kz
[3]Мирзоян М.,
PhD, ORCID ID: 0000-0002-1474-8330,
e-mail: mojtaba.mirzaeian@uws.ac.uk
[1]Абдуллин Х.А.,
ф.-м.ғ.д., профессор, ORCID ID: 0000-0002-2729-2272,
e-mail: kh.abdullin@physics.kz

[1]Әл-Фараби атындағы Қазақ ұлттық университеті, Алматы қ., Қазақстан
[2]Білім беру және гуманитарлық ғылымдар мектебі, СДУ Университеті,
Қаскелең қ., Қазақстан
[3]Есептеу техникасы, инженерия және физикалық ғылымдар мектебі,
Батыс Шотландия университеті, Пейсли қ., Ұлыбритания

ГИБРИДТІ СУПЕРКОНДЕНСАТОРЛАРҒА АРНАЛҒАН NI_3S_2/NI КӨБІК ЭЛЕКТРОДТАРЫНЫҢ БЕТКІ ТҮРЛЕНУІ ЖӘНЕ ЖАҚСАРТЫЛҒАН ЭЛЕКТРОХИМИЯЛЫҚ СИПАТТАМАЛАРЫ

Аңдатпа

Никель көбігінің бетін сульфидтеу процесі жоғары электрохимиялық сыйымдылығы және электрохимиялық циклдеу кезінде жоғары тұрақтылығы бар Ni_3S_2 қабаттарын алу мақсатында жан-жақты зерттелді. Алайда электрохимиялық жұмыс жағдайларында Ni_3S_2/NF (никель көбігі) электродында түзіледі деп болжанатын никель гидроксиді қабаттарының рөлі әлі күнге дейін жеткілікті деңгейде зерттелмеген. Осы жұмыста гидроксидтік фазаның электрохимиялық сыйымдылыққа да, циклдік тұрақтылыққа да елеулі үлес қосатыны көрсетілді. Ni_3S_2/NF электроды тиомочевина қатысында 160 °C температурада бірсатылы гидротермалдық әдіспен дайындалды. NF бетінде бастапқыда түзілген Ni_3S_2 құрылымы кейіннен KOH электролитінде электрохимиялық циклдеу нәтижесінде модификацияланды. Электродтың электрохимиялық сыйымдылығының артуы бірнеше никель гидроксиді фазаларының түзілуімен қатар жүрді, бұл рентгендік дифракция (XRD) және Раман спектроскопиясы әдістерімен расталды. Электрод 20 $А \cdot г^{-1}$ ток тығыздығында жүргізілген 20 000 гальваностатикалық заряд-разряд (GCD) циклі барысында максималды сыйымдылығының 90%-ын сақтап, жоғары циклдік тұрақтылық көрсетті. Ni_3S_2 электродының меншікті сыйымдылығы 2,7 $А \cdot г^{-1}$ ток тығыздығында 758 $Ф \cdot г^{-1}$ құрады. Ток тығыздығы 90 $А \cdot г^{-1}$-ге дейін арттырылған кезде меншікті сыйымдылық 233 $Ф \cdot г^{-1}$-ге дейін төмендеді, бұл 2,7 $А \cdot г^{-1}$ ток тығыздығындағы мәннің шамамен 30%-ын құрайды.

Түйін сөздер: Ni_3S_2, никель көбігі, гибридті суперконденсатор, никель гидроксиді, электрохимиялық белсендіру, циклдік тұрақтылық.

[1]Канатов Ж.С.,
PhD студент, ORCID ID: 0009-0003-2975-0999,
kanatovzhantilek@gmail.com
[1*]Калкозова Ж.К.,
к.ф.-м.н., профессор, ORCID ID: 0000-0002-4826-1678,
*e-mail: zhanar.kalkozova@kaznu.edu.kz
[2]Мұқаш Ж.О.,
PhD, Ассистент профессор, ORCID ID: 0009-0004-7713-3925,
e-mail: zhanar.mukash@sdu.edu.kz
[3]Мирзоян М.
PhD, ORCID ID: 0000-0002-1474-8330,
e-mail: mojtaba.mirzaeian@uws.ac.uk
[1]Абдуллин Х.А.,
д.ф.-м.н., профессор, ORCID ID: 0000-0002-2729-2272,
e-mail: kh.abdullin@physics.kz

[1]Национальная нанотехнологическая лаборатория открытого типа,
Казахский национальный университет им. аль-Фараби, г. Алматы, Казахстан
[2]Школа образования и гуманитарных наук, Университет СДУ, г. Каскелен, Казахстан
[3]Школа вычислительной техники, инженерии и физических наук,
Университет Западной Шотландии, г. Пейсли, Великобритания

ПРЕОБРАЗОВАНИЕ ПОВЕРХНОСТИ И УЛУЧШЕННЫЕ ЭЛЕКТРОХИМИЧЕСКИЕ ХАРАКТЕРИСТИКИ ЭЛЕКТРОДОВ NI_3S_2/NI ПЕНЫ ДЛЯ ГИБРИДНЫХ СУПЕРКОНДЕНСАТОРОВ

Аннотация

Процесс сульфидирования поверхности никелевой пены для получения слоёв Ni_3S_2 с высокой электрохимической емкостью и стабильностью при электрохимическом циклировании, был подробно изучен. Однако роль слоев гидроксида никеля, которые, как предполагается, образуются в условиях электрохимической работы электрода Ni_3S_2/NF (никелевая пена), до сих пор не была достаточно изучена. В настоящей работе показано, что гидроксидная фаза вносит значительный вклад как в электрохимическую емкость, так и в циклическую стабильность. Электрод Ni3S2/NF был изготовлен с помощью одноэтапного гидротермального метода в присутствии тиомочевины при температуре 160 °C. Первоначальная структура Ni_3S_2 на поверхности NF впоследствии была модифицирована в результате электрохимических циклов в электролите KOH. Увеличение электрохимической емкости электрода сопровождалось образованием нескольких фаз гидроксида никеля, что было подтверждено с помощью рентгеновской дифракции (XRD) и рамановской спектроскопии. Электрод продемонстрировал высокую стабильность характеристик в течение 20 000 циклов гальваностатического заряда-разряда (GCD) при плотности тока 20 $А·г^{-1}$, сохранив 90% своей максимальной емкости. Удельная ёмкость электрода Ni3S2 составила 758 $Ф·г^{-1}$ при плотности тока 2,7 $А·г^{-1}$. При увеличении плотности тока до 90 $А·г^{-1}$ удельная емкость снизилась до 233 $Ф·г^{-1}$, что составляет 30% от значения при плотности тока 2,7 $А·г^{-1}$

Ключевые слова: Ni_3S_2, никелевая пена, гибридный суперконденсатор, гидроксид никеля, электрохимическая активация, циклическая стабильность.